Technical Note: Time-gating to medical linear accelerator pulses: Stray radiation detector

Muhammad Ramish Ashraf[a)] and Petr Bruza
Thayer School of Engineering, Dartmouth College, Hanover, NH 03755, USA

Venkat Krishnaswamy
Thayer School of Engineering, Dartmouth College, Hanover, NH 03755, USA
DoseOptics LLC, Lebanon, NH 03766, USA

David J. Gladstone
Thayer School of Engineering, Dartmouth College, Hanover, NH 03755, USA
Department of Medicine, Geisel School of Medicine, Dartmouth College Hanover, Hanover, NH 03755, USA
Norris Cotton Cancer Center, Dartmouth-Hitchcock Medical Center, Lebanon, NH 03756, USA

Brian W. Pogue
Thayer School of Engineering, Dartmouth College, Hanover, NH 03755, USA
DoseOptics LLC, Lebanon, NH 03766, USA

(Received 21 May 2018; revised 5 November 2018; accepted for publication 21 November 2018; published 14 December 2018)

Purpose: CCD cameras are employed to image scintillation and Cherenkov radiation in external beam radiotherapy. This is achieved by gating the camera to the linear accelerator (Linac) output. A direct output signal line from the linac is not always accessible and even in cases where such a signal is accessible, a physical wire connected to the output port can potentially alter Linac performance through electrical feedback. A scintillating detector for stray radiation inside the Linac room was developed to remotely time-gate to linac pulses for camera-based dosimetry.
Methods: A scintillator coupled silicon photomultiplier detector was optimized and systematically tested for location sensitivity and for use with both x rays and electron beams, at different energies and field sizes. Cherenkov radiation emitted due to static photon beams was captured using the remote trigger and compared to the images captured using a wired trigger. The issue of false-positive event detection, due to additional neutron activated products with high energy beams, was addressed.
Results: The designed circuit provided voltage >2.5 V even for distances up to 3 m from the isocenter with a 6 MV, 5 × 5 cm beam, using a Ø3 × 20 mm^3 $Bi_4Ge_3O_{12}$ (BGO) crystal. With a larger scintillator size, the detector could be placed even beyond 3 m distance. False-positive triggering was reduced by a coincidence detection scheme. Negligible fluctuations were observed in time-gated imaging of Cherenkov intensity emitted from a water phantom, when comparing directly connected vs this remote triggering approach.
Conclusion: The remote detector provides untethered synchronization to linac pulses. It is especially useful for remote Cherenkov imaging or remote scintillator dosimetry imaging during radiotherapeutic procedures when a direct line signal is not accessible. © *2018 American Association of Physicists in Medicine* [https://doi.org/10.1002/mp.13311]

Key words: time-gated acquistion, linac, cherenkov, scintillation

1. INTRODUCTION

Diagnostic devices that are synchronized to the medical linear accelerator (linac) can be used to track events resulting from linac radiation pulses. Medical linacs deliver x ray or electron beam pulses of 3–6 μs duration with a 60–360 Hz repetition rate. One useful feature of this low duty cycle delivery is that light emitted from scintillators placed in the beam can be sampled for dosimetric purpose, at this same frequency, thereby removing considerable ambient background.[1] Time-gated optical imaging can also be used to image Cherenkov Radiation.[2,3] The underlying principle in these diagnostic measurements makes use of the pulsed nature of linac output and time-gated image acquisition. As a side effect of the beam generation and dose delivery, pulsed stray x-ray radiation is emitted from the beam target. Minor x-ray leakage from the linac gantry is also expected. In both cases, the waveform of the stray radiation follows the waveform of the primary x ray or electron beam, and thus can be used for remote beam detection. In this work, a trigger circuit for detection of stray radiation was prototyped and optimized. Finally, the detector was compared against wired triggering.

Most Linac vendors provide service access to signals that make time-gating possible for research purposes. Two such signals are the target current signal port (TargI) and the Klystron Voltage (KlyV) port. The TargI signal provides a high voltage pulse only when the electron beam hits a tungsten target in the gantry head and produces bremsstrahlung radiation.

Since the electron beam is pulsed, the TargI port can be used for time-gating to the linac pulses. A long BNC cable can be used to connect the TargI or the KlyV port from the linac control unit to the external trigger port of the camera. However, a physical trigger cable can induce an unwanted electronic feedback or an impedance change to the linac circuitry, which can potentially alter the charge distribution or current flow at the target. It is also common that manufacturer may limit access to the linac's control unit, thereby making time-gated image acquisition hard to achieve.

To overcome these issues, we proposed a method of remote triggering by a stray radiation detector. A silicon photomultiplier tube (SiPM) module was coupled to a scintillator which operates by detection of stray radiation inside the linac room. As ionizing radiation impinges on the scintillator crystal, optical radiation is emitted from the crystal. These scintillation photons are then detected by the SiPM module and converted into a voltage pulse by current-to-voltage amplifier. This voltage pulse can be used to trigger the time-gated Cherenkov imaging camera. This approach requires no physical wire connection to the linac and has the potential to provide remote synchronization to linac pulses in cases when service signals such as the TargI and KlyV are not accessible. Moreover, such a wireless trigger would allow more flexibility in terms of camera placement inside the linac bunker.

2. MATERIALS AND METHODS

2.A. Feasibility study

As an initial feasibility study, the detector was placed at different locations inside the linac bunker and tested with beams of different sizes and energies. The detector output at each location and beam energy and size was noted. A schematic of the experimental setup in shown in Fig. 1(a) and a characteristic waveform observed on a digital sampling oscilloscope (PicoScope 3406D, Cambridgeshire, UK) is shown in Fig. 1(b). A $Bi_4Ge_3O_{12}$ (BGO) crystal (EPIC Crystal, Kunshan, China) was coupled to C13365-3050SA silicon photomultiplier (SiPM) module (Hamamatsu Photonics, Shizuoka, Japan) to detect stray x-ray radiation from medical linac (Varian 2100CD, Palo Alto, CA, USA). The crystals' surface outside the SiPM windows were wrapped in white Teflon tape and optically shielded by an opaque plastic enclosure to eliminate stray light detection. Two different configurations of the scintillating crystal were used. For quantitative assessment of the peak output voltages at various room locations and beam parameters, we used a smaller scintillator ($Ø3 \times 20$ mm^3) with an additional thin neutral density (ND) filter (optical density 1.0) between the crystal and detector. In the second configuration, an array of eight $5 \times 5 \times 5$ cm^3 BGO crystals was employed. This configuration produces a scintillation light output that always saturates the SiPM sensor irrespective of the trigger's location within the room, beam energy, or beam size. Such a configuration would be the most effective as a trigger for the camera. We assume 2.5 V threshold to indicate the leading edge of trigger signal, which is half of the maximum amplitude that can be provided by SiPM module and is also compatible with the voltage level of transistor-transistor logic. SiPM module output was recorded along with Klystron current (KlyI) and TargI service signals. The typical recorded waveforms are shown in Fig. 2(b). During measurements, a $30 \times 30 \times 15$ cm block of Solid Water (Sun Nuclear, Melbourne, FL, USA) was used as a dose delivery phantom.

At higher energies (≥10 MV), neutron activated products are formed. The neutron activated products decay at their own rate and produce spurious pulses and false triggers. A coincidence detection mechanism was investigated to circumvent the issue of false triggering. We proposed to use a single AND gate that accepts input from two different detectors and performs logical summation of the inputs. The output of the gate is then used to trigger the intensifier driver. The block schematic and a photograph of our implementation is shown in Fig. 2.

2.B. Time-gated imaging

Cherenkov emission from a 12.7 cm diameter × 30.5 cm deep cylindrical water phantom doped with quinine sulfate (1 g/L) was then captured using a 20 m physical trigger cable and the detector as trigger signals for an intensified CMOS camera (DoseOptics, Lebanon, NH, USA). The camera was equipped with an 135 mm f/2 lens (Canon USA Inc., Melville, NY, USA). The midpoint of the cylindrical phantom was aligned to the isocenter. A static 6 MV, 100 Monitor Units (MU), 600 MU/min (360 Hz pulse repetition rate), 5×5 cm^2 beam was delivered with the gantry rotated to 90 degrees. For this study, the 2100CD linac (Varian, Palo Alto, CA, USA) was used. The camera and detector were placed at 2 m from the phantom. CMOS gain was set to 400 and the exposure time was set to 15 ms. The intensifier was gated by the external or stray x ray trigger signal for a preset duration of 4 μs. Therefore, the CMOS imaging sensor will collect light only during a delivery of a radiation pulse by the linac. Using 15 ms exposure time, we collected five linac pulses in a single frame. Spatial and temporal median filter were then applied over the stack of images. The stack of images was then averaged to obtain one single frame. A frame by frame analysis was performed and the final averaged frame was compared for the remote detector and the wired trigger. The array of eight $5 \times 5 \times 5$ cm^3 BGO crystals was used in the remote detector for this experiment.

3. RESULTS

3.A. Feasibility study

For Fig. 3, the $Ø3 \times 20$ mm^3 scintillator with the thin ND filter (optical density 1.0) was used. The peak voltage ratio of the large scintillator to the small scintillator detector was found to be approximately 70. Figure 3(a) shows the detector output as a function of the distance of the detector

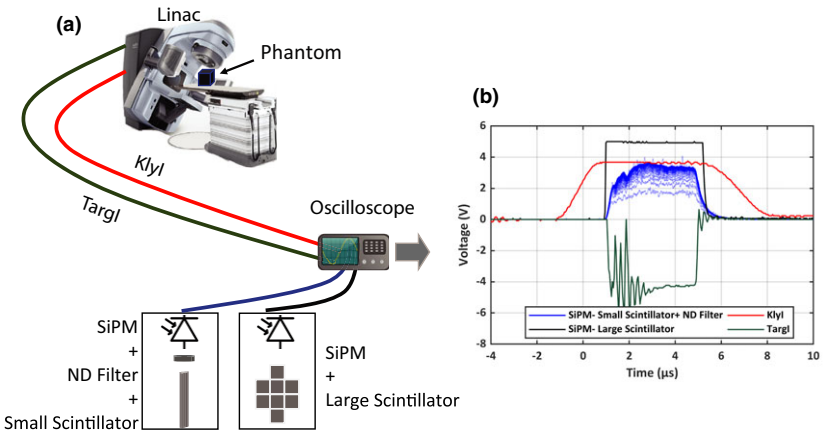

FIG. 1. (a) A schematic of the experimental setup. A medical linear accelerator was used to deliver radiation to a 30 × 30 × 15 cm block of solid water. Two synchronization signals, Klystron current (KlyI) and Target current (TargI) from the linac were connected to a digital oscilloscope using a BNC cable. Two different scintillation configurations were used; 1) An array of eight 5 × 5 × 5 cm^3 BGO crystals; 2) Ø3 × 20 mm^3 BGO Crystal and a thin neutral density filter (OD 1.0) (not shown in figure). (b) Characteristic waveforms and timing of X-ray trigger output and linac service signals (KlyI and TargI), are shown in persistence mode (total number of pulses: 100). [Color figure can be viewed at wileyonlinelibrary.com]

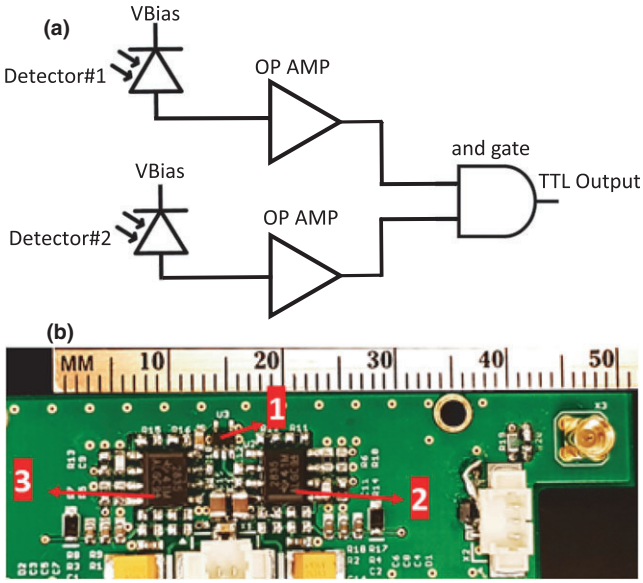

FIG. 2. (a) Block diagram of the coincidence detection circuit. The circuit takes input from two different detector, amplifies, and performs logical AND operation on them. (b) Realization of the circuit where 1) is the logical AND gate and 2) and 3) are operational amplifiers. [Color figure can be viewed at wileyonlinelibrary.com]

from the isocenter. 6 MV and 6 MeV 10 × 10 cm^2 beams were used for photons and electrons, respectively. The detector output decreases as the detector moves away from the isocenter. At 3.0 m, an amplitude of 0.5 V (6 MV photon beam) or 0.2 V (6 MeV electrons) was detected, corresponding to theoretical 35 and 14 V amplitudes in large scintillator detector, respectively. Therefore, even at 3.0 m from the isocenter, the detector provides enough voltage for both photon and electron beams.

To assess the detector output for different beam sizes, we placed the detector 2.0 m from the isocenter and varied the beam size from 5 × 5 to 25 × 25 cm^2. About 6 MV and 6 MeV beams were used for photons and electrons, respectively. While the photon beam shows a linear increase in detector output with increasing beam size, the increasing electron beam sizes result in only a slight increase in detector output. Extrapolated amplitude of approximately 0.4 V at zero beam size [Fig 3(b)] suggests a presence of stray radiation even with fully closed jaws during both electron and photon deliveries. This signal is most likely present due to radiation leakage from the bending magnet assembly in the gantry. Amplitude of this signal from small scintillator detector corresponds to a theoretical amplitude of 28 V in large scintillator detector, which is again well above the threshold level.

Detector output for 10 × 10 cm^2 radiotherapeutic beams of different energies and types (photons vs. electrons) was also measured. The detector was placed at 2.0 m from the isocenter. The average amplitude of the detector with the small scintillator was 1.1 ± 0.4 V. Using the small scintillator to large scintillator conversion ratio, the theoretical peak voltage of large scintillator detector comes out to be approximately 77 V, well above the 2.5 V threshold level. The remote trigger was also observed to trigger a few hundreds of nanoseconds before the wired trigger. For a 6 MV photon beam, at 0.5 m distance, the stray radiation detector signal would trigger 132 ns before the TargI signal. As the distance between the detector and the isocenter increases, this time difference decreases to 85 ns at 3.0 m distance.

3.B. Coincidence-based triggering

Delayed, short yet intense scintillation pulses were detected after each 18 MV photon pulse and to a lesser extent, after 15 and 18 MeV electron beam pulses. These pulses, generated most likely by neutron activation products, may result in false-positive triggering of the time-gated equipment. A coincidence detection mechanism can be

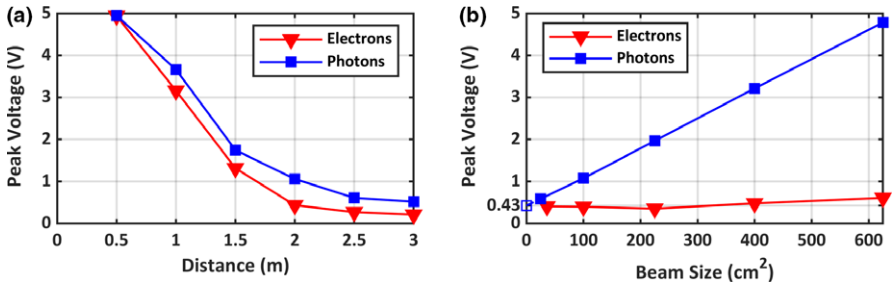

FIG. 3. (a) Detector output as a function of distance from the isocenter for a 6 MV/6 MeV, 10 × 10 cm^2 beam. (b) Detector output as a function of beam size at 2.0 m away from the isocenter with a 6 MV and a 6 MeV beam [Color figure can be viewed at wileyonlinelibrary.com]

employed to overcome this issue. The probability of detecting two spurious pulses simultaneously with two different detectors is low. Thus, this can be overcome using a coincidence detection. This was implemented by performing logical AND operation on output of the two different detectors. In Fig. 4, TargI, response from two different detector and the final output of the AND gate are shown. The resulting final waveform shows that the unwanted false positive events were eliminated. Negligible delay was induced the in the trigger signal due to the added components.

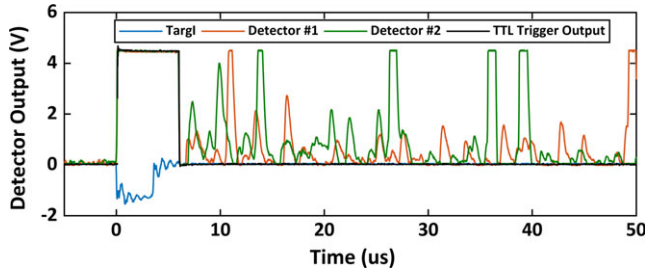

FIG. 4. Scintillation response of the two detectors to X-ray beam pulse and additional spurious pulses after the delivery of the beam. The final output is obtained after performing logical AND operation on the output of the two detectors. The final TTL output does not suffer from spurious pulses. [Color figure can be viewed at wileyonlinelibrary.com]

3.C. Time-gated imaging

A 6 MV, 100 MU, 600 MU/min, 5 × 5 cm^2 beam was delivered to the cylindrical water (doped with 1 g/L quinine) phantom with the gantry head rotated to 90°. 100 MUs at a dose rate of 600 MU/min should result in an acquisition time of ~10 s. This was confirmed when the total acquisition time came out to be about 10.07 s for both the wired and the remote trigger. Additionally, a dose rate of 600 MU/min translates into a pulse period of 2.778 ms (i.e., 360 Hz repetition rate). With an exposure time of 15 ms, five linac pulses per each frame are expected. For both the remote and the wired trigger, the total number of frames came out to be 605. Final averaged image of the 605 image stack is shown in Fig. 5 for both the wired and detector triggered acquisitions. The figure shows that the image captured using the detector has negligible differences compared to the one captured using the TargI as the trigger source. For the two modalities, a difference of <1.5% of the cumulative intensity was observed in the Cherenkov emission.

It is also imperative that a frame by frame analysis be performed to see how the intensity varies with time for each modality. Such a comparison is presented in Fig. 6. A rectangular region of interest (ROI), that was constant across both frames within and across the two datasets, was chosen around the midpoint of the beam axis. The average pixel intensity in the ROI was computed for each frame. Figure 6(a) shows frame by frame variation in average pixel intensity for both the TargI and the Wireless detector as trigger sources. The agreement between TargI and the remote detector is again within 1%. Figure 6(b) shows the relative percentage difference between the two plots with the TargI data as the reference. The average ROI pixel intensity for the remote detector was on average 0.9% greater than the corresponding average ROI pixel intensity for TargI.

4. DISCUSSION

To act as a trigger for the camera, the detector should be able to trigger the camera independent of the beam type, energy, size used, and the location of the camera in the room. Our experiments show that within the typical operating ranges of linac and large scintillator detector, the stray x-ray radiation produced ample scintillation signal that can be used for linac-synchronized time-gating. Depending on the location of the detector in the linac room, beam size, and beam energy, the stray radiation due to photon beams produced 1–8 times larger scintillator output than in the case of electron beams.

A linear increase in detector output was observed for increasing photon beam size, whereas for electrons, the detector output was nearly constant around 0.4 V baseline. The origin of baseline signal may be explained by a nearly constant x-ray leakage from linac head — most likely the electron bending magnet shielding — before beam collimation and shaping. Increase in signal from increasing x-ray beam size can be attributed to increased scatter from the irradiated phantom and the floor. The signal during electron beam radiation is most likely due to x-ray production in the head of the accelerator. Sources include the bending magnet, the primary collimating jaws, and the secondary electron skimmers in the cone assembly; all but the latter stay constant with chosen electron field size.

Since the amplitude of the detector output depends largely on the size of the scintillating material, one could use larger

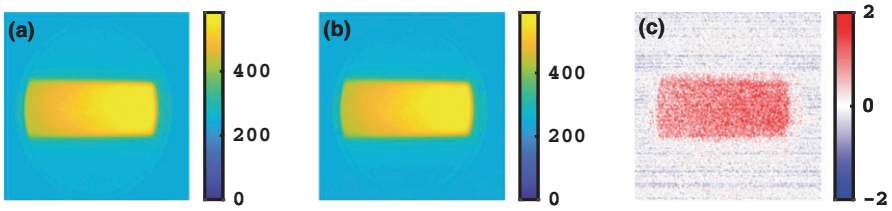

FIG. 5. Cherenkov emission from a cylindrical water phantom doped with 1 g/L quinine sulfate captured using an intensified CMOS camera with (a) the TargI and (b) Remote detector as trigger signals. A 6 MV, 100 MU, 600 MU/min, 5 × 5 cm^2 beam was used. (c) The relative percentage difference between images (a) and (b). The TargI image was considered as the baseline in this case. [Color figure can be viewed at wileyonlinelibrary.com]

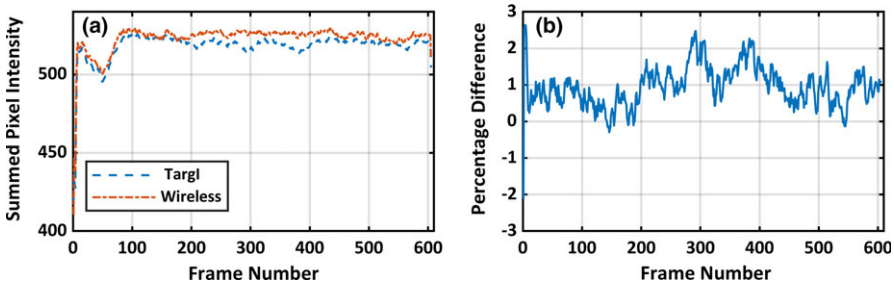

FIG. 6. (a) Average pixel intensity for a ROI chosen around the midpoint of the cylindrical water phantom for TargI and the Remote detector with the static 6 MV 100 MU, 600 MU/min beam. (b) Percentage difference between the average pixel intensity captured using TargI and the remote detector. [Color figure can be viewed at wileyonlinelibrary.com]

scintillator to trigger any time-gated equipment even at extreme locations inside the room. However, use of larger scintillators would result in higher probability of detecting stray β and γ-rays, generated during decay of radioisotopes that were created by [γ, n] and [n, γ] reactions in the linac head and all irradiated objects.[4,5] In practice, this would have resulted in false-positive trigger events. We demonstrated that the coincidence-based detection effectively.

Small Cherenkov intensity discrepancy (<1.5%) was observed between images captured using the remote detector and TargI as a trigger for a static 6 MV beam. The fact that the remote detector captures 1.5% more Cherenkov intensity may be explained by the delay that is induced in the TargI signal because of the cable-specific delay. However, this phenomenon is location specific and only valid if the transmission line is longer than the line-of-sight between the remote trigger and gantry/irradiated object. In this study, a 20 m cable was used which is longer than the line-of-sight and the remote trigger was 2 m away from the gantry head.

5. CONCLUSION

Our stray radiation triggering module provides an electric signal which is synchronized to pulses of radiotherapy linac beams of various field sizes and energies. The detector is particularly useful for remote Cherenkov imaging or remote scintillator dosimetry imaging. This module overcomes the delay caused by wire-based triggering and eliminates the limitations for interfacing medical devices.

ACKNOWLEDGMENTS

This work has been sponsored by National Institutes of Health research grants R44 CA199681, R01 EB023909, R01 EB024498, and P30 CA 23108.

CONFLICTS OF INTEREST

The authors have no relevant conflicts of interest to disclose.

[a]Author to whom correspondence should be addressed. Electronic mail: muhammad.ramish.ashraf.th@dartmouth.edu..

REFERENCES

1. Jarvis L, Zhang R, Gladstone D, et al. Cherenkov video imaging allows for the first visualization of radiation therapy in real time. *Int J Radiat Oncol Biol Phys*. 2014;89:615–622.
2. Glaser A, Zhang R, Davis S, Gladstone D, Pogue B. Time-gated Cherenkov emission spectroscopy from linear accelerator irradiation of tissue phantoms. *Opt Lett*. 2012;37:1193.
3. Čerenkov P. Visible radiation produced by electrons moving in a medium with velocities exceeding that of light. *Phys Rev*. 1937;52:378–379.
4. Fischer H, Tabot B, Poppe B. Activation processes in a medical linear accelerator and spatial distribution of activation products. *Phys Med Biol*. 2006;51:N461–N466.
5. Howell R, Kry S, Burgett E, Hertel N, Followill D. Secondary neutron spectra from modern Varian, Siemens, and Elekta linacs with multileaf collimators. *Med Phys*. 2009;36:4027–4038.